

Thermal transport in long-range interacting Fermi-Pasta-Ulam chains

Jianjin Wang,¹ Sergey V. Dmitriev,^{2,3} and Daxing Xiong^{4,*}

¹*Department of Physics, Jiangxi Science and Technology Normal University,
Nanchang 330013, Jiangxi and Department of Physics,
Fuzhou University, Fuzhou 350108, Fujian, China*

²*Institute for Metal Superplasticity Problems of RAS, Khalturin Street 39, 450001 Ufa, Russia*

³*Institute of Mathematics with Computing Centre,
the Ufa Federal Research Centre of RAS, Chernyshevsky Street 112, 450008 Ufa, Russia*

⁴*School of Science, Jimei University, Xiamen 361021 and Department of Physics,
Fuzhou University, Fuzhou 350108, Fujian, China*

Studies of thermal transport in long-range (LR) interacting systems are currently particularly challenging. The main difficulties lie in the choice of boundary conditions and the definition of heat current when driving systems in an out-of-equilibrium state by the usual thermal reservoirs. Here, by employing a reverse type of thermal baths that can overcome such difficulties, we reveal the intrinsic features of thermal transport underlying a LR interacting Fermi-Pasta-Ulam chain. We find that under an appropriate range value of LR exponent $\sigma = 2$, while a *nonballistic* power-law length (L) divergence of thermal conductivity κ , i.e., $\kappa \sim L^\alpha$ still persists, its scaling exponent $\alpha \simeq 0.7$ can be much larger than the usual predictions in short-range interacting systems. The underlying mechanism is related to the system's new heat diffusion process, weaker nonintegrability and peculiar dynamics of traveling discrete breathers. Our results shed light on searching for low-dimensional materials supporting higher thermal conductivity by involving appropriate LR interactions.

I. INTRODUCTION

Thermal transport in one-dimensional (1D) systems has been a topic of both theoretical and practical interest for several decades [1–3]. One of the main achievements has been to realize that most 1D systems can display anomalous behaviors. This anomaly means that the “standard” thermal transfer law, i.e., Fourier’s law, $J = -\kappa \nabla T$, which states that heat current J is proportional to temperature gradient ∇T with κ the thermal conductivity being constant for a bulk material, is not valid. Instead, κ shows a sublinear power-law divergence as increasing system size L , i.e., $\kappa \sim L^\alpha$ ($0 < \alpha < 1$). This issue is in part motivated by the recent carbon nanotubes (CNTs) technology [4, 5], and also by the desire to understand the microscopic origin of non-Fourier’s thermal transport. Additionally, a fascinating topic of efficiently controlling heat has led to the emerging field of phononics [6–10]. Nevertheless, despite these achievements and the practical importance, our main theoretical understandings are based on the 1D anharmonic chains with nearest-neighbor (NN) couplings, whose interactions are short-range (SR). How thermal transport would behave in long-range (LR) interacting systems is an open fundamental question.

LR interactions are usually characterized by potential $V(r)$ decays with the distance r between two particles in a power law $V(r) \propto r^{-\sigma}$, where σ denotes the range of interaction. Generally, the cases of σ lower than the system’s spatial dimension (in 1D systems, $\sigma < 1$)

are called as the LR-interacting systems [11, 12]. Such LR-interactions are ubiquitous in several physical systems, ranging from self-gravitating to nanoscale, and to quantum systems [11–14]. These LR interacting systems can display peculiar features, such as ensemble inequivalence [12], anomalous diffusion of energy [13] and lack of additivity [14]. The nonadditivity means that even in the thermodynamic limit, to decompose an initial equilibrium system into two effectively noninteracting subsystems is impossible. As a result, when one deals with thermal transport by coupling the usual thermal reservoirs to two ends of the system [15], the central bulk system and the two thermalized ends are implicitly identified. Eventually, the whole system may display properties that do not correspond to the original one. In this respect one does not know how to choose the boundary conditions and define the heat current [16]. This difficulty has limited our understanding of thermal transport of a true LR interacting system [16–22].

In this article we aim to reveal the intrinsic feature of thermal transport underlying a LR interacting chain. Toward that end and following [16–22], we use the terminology of LR interactions in a wider sense regardless of the range exponent σ . This means that we regarding systems with all σ values as the generalized LR interacting systems. One might immediately recognize that for $\sigma \geq 1$ the nonadditivity will not appear, however, we stress that in studies of thermal transport, the difficulties of choice of the boundary conditions and definition of heat current still persist when one applies the usual thermal reservoirs. To solve these difficulties, we here instead employ a “reverse nonequilibrium molecular dynamics (RNEMD)” method [23, 24] to build the nonequilibrium stationary state. This method is advantageous since it can get rid of the problem of boundary

*Electronic address: xmuxdx@163.com; Electronic address: phyxiongdx@fzu.edu.cn

effects. Besides, as shown below, the definition of heat current is natural. With this advantage we are able to reveal that a length-divergence exponent of $\alpha \simeq 0.7$, which is much larger than the original theoretical predictions ($\alpha \simeq 0.2-0.5$, see [1–3, 25, 26]), can be achieved in a theoretical model of the LR interacting Fermi-Pasta-Ulam (FPU) chain under an appropriate range value $\sigma = 2$. This provides the theoretical possibility of producing a higher α ($\alpha \simeq 0.6-0.8$) [4, 27, 28] by including suitable LR interactions. This also suggests the need to extend the study of thermal transport in systems beyond SR interactions [22]. In principle, this implies new mechanisms for transport.

Before proceeding, we would also like to emphasize that the present technology already allows us to fabricate materials with LR interactions. The Coulomb crystals [29], Ising pyrochlore magnets [30, 31], and permalloy nanomagnets [32] are some of the notable examples. Highly efficient thermal rectification has recently been achieved in systems involving LR interactions [33, 34].

II. MODELS

We consider a FPU type LR interacting chain of N particles with Born-von Karman periodic boundary condition [35] whose dynamics is governed by the Hamiltonian [36]:

$$H = \sum_i^N \left[\frac{p_i^2}{2} + \frac{1}{2} \sum_{j \neq i}^N \frac{(x_j - x_i)^2}{(r_{ij})^{\sigma'}} + \frac{1}{4} \sum_{j \neq i}^N \frac{(x_j - x_i)^4}{(r_{ij})^\sigma} \right]. \quad (1)$$

Here, both the particle's mass and lattice constant are set to be unity and all the relevant quantities are dimensionless; x_i and p_i are two canonically conjugated variables with i the index of the particle; $(r_{ij})^{\sigma'(\sigma)}$ represents the interaction strength of the i th particle with its $|j - i|$ th neighbors with $\sigma'(\sigma)$ the range value of LR exponent. r_{ij} is the shortest distance between particles i and j on this periodic chain, and we define

$$r_{ij} = \begin{cases} 0, & i = j, \\ |j - i|, & 1 \leq |j - i| \leq N/2, \\ N - |j - i|, & N/2 + 1 \leq |j - i| \leq N - 1. \end{cases} \quad (2)$$

We do not include the Kac scaling factors $\tilde{N}'(\tilde{N}) = \frac{1}{N} \sum_{i=1}^N \sum_{j \neq i}^N (r_{ij})^{-\sigma'(-\sigma)}$. These factors were designed to restore the system's extensivity as increasing system size, but it does not help improve the system's nonadditivity [13]. It only constructs an "artificial" extensive system, but the cost for thermal transport is that both the phonon's group velocity and the strength of nonlinearity should depend on N , which is an unwanted effect. In fact, if one looks at dynamical aspects, for a correspondence between both treatments, the difference is that time should be $\tilde{N}^{1/2}$ scaled (setting $\tilde{N}' = \tilde{N}$) [37].

We shall focus on the case of $\sigma = 2$ ($\sigma' = \infty$) and also present the result of $\sigma = 8$ ($\sigma' = \infty$) for comparison. This only involves the LR interactions in the quartic anharmonic term [19], which differs from the model in [16], but we have confirmed that it does not violate our general conclusion [38]. $\sigma = 8$ might correspond to the original FPU model with NN interactions, although this equivalence requires $\sigma \rightarrow \infty$. The case of $\sigma = 2$ is particularly interesting since in this case ballistic transport ($\alpha \simeq 1$) [16, 19], like that observed in integrable systems [39, 40], has been conjectured. As the anharmonicity will generally cause nonintegrability, one might attribute such observed integrable dynamics to the strong finite-size effects suffered from using the usual thermal reservoirs [15] and including the Kac scaling factors. Indeed, it has been pointed out, due to this, that to gain convincing results for $\sigma = 2$ is extremely hard [16]. But anyway, as shown in the following, this implies new physics. Another point for $\sigma = 2$ of interest is that the system under zero temperature can support tail-free traveling discrete breathers (DBs) [41]. Then one might ask, what will happen to these moving excitations under finite-temperature systems and how would they affect transport? Addressing this would also invoke the broad interest of the DB field.

III. METHOD

The RNEMD method produces a temperature gradient in a reverse way. Unlike the traditional approach [15] to directly induce ∇T , it imposes the heat current by frequently exchanging particle kinetic energy (or momentum). While the nonequilibrium stationary state is reached, ∇T will be established. This "reversion" makes the RNEMD method an ideal candidate for studying thermal transport in LR interacting systems. We also note that the vasp [42] and lammps [43] codes modified to such method have been widely used.

We implement the method in this way: First, since the Born-von Karman periodic boundary condition is used, the chain forms like a ring. We decompose the ring into $M = 32$ equal slabs (each contains $n = N/M$ particles). We give each slab a serial number k and label the cold one slab 1 and accordingly, the hot one slab $M/2 + 1$. This labeling allows us to interchange the momentum of the hottest particle in slab 1 with that of the coldest particle in slab $M/2 + 1$ at a frequency $f_{exc} = 0.1$. Such interchanges cause a redistribution of kinetic energy of the system with an energy difference: $\Delta E = \sum \frac{p_h^2 - p_c^2}{2}$ during time t , where the subscripts h and c refer to the hottest and coldest particles whose momenta are exchanged, and the sum runs over all exchange events in time t . As a consequence, the relaxation of energy difference will drive two heat currents to flow from hot to cold slabs along the two semi-ring sides bridging them (each side has an effective length $L = N/2 - n$). After the stationary state is eventually reached, the long-time averaged

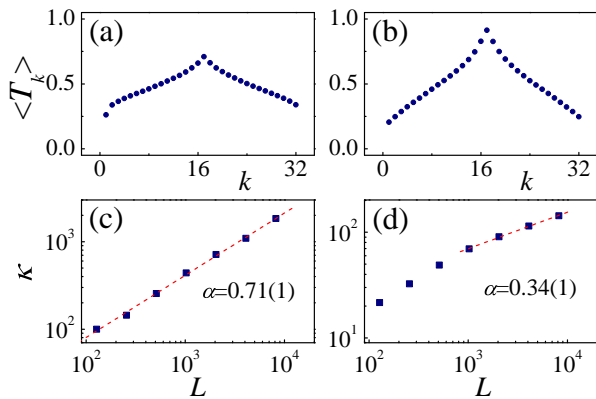


FIG. 1: Temperature profile over slabs for $\sigma = 2$ (a) and 8 (b) with $L = 7680$ ($N = 16384$). κ vs L for $\sigma = 2$ (c) and 8 (d). The dashed lines denote $\kappa \sim L^\alpha$, suggesting $\alpha = 0.71 \pm 0.01$ (0.34 ± 0.01) for $\sigma = 2$ (c) [8 (d)].

current across each side is defined by $\langle J \rangle = \lim_{t \rightarrow \infty} \frac{\Delta E}{2t}$; accordingly the time averaged kinetic temperature of slab k is $\langle T_k \rangle = \frac{1}{nk_B} \sum_{i=n(k-1)+1}^{nk} p_i^2$, where k_B is the Boltzmann constant (set to unity) and the sum runs over all n particles in slab k . The heat conductivity κ can then be obtained by $\kappa = -\langle J \rangle / \nabla T$ according to Fourier's law, with ∇T being evaluated over the slabs between the cold and hot ones.

We start calculations with several fully thermalized systems under $T = 0.5$. These systems are evolved by the velocity-Verlet algorithm [44] with a small time step 0.01, that guarantees energy conservation with a relative accuracy of $O(10^{-5})$. We adopt a Fast Fourier Transform (FFT) [45] algorithm to accelerate our computations. This helps avoid $O(N^2)$ operations in calculating forces at each time step in LR interacting systems. With this, a transient time 10^6 for the system to reach the stationary state, is discarded, and another evolution time 10^6 is performed for the average.

IV. MAIN RESULTS

Figures 1(a,b) depict two typical temperature profiles over slabs for $\sigma = 2$ and 8. In both cases a well-behaved temperature gradient is identified. The difference is that ∇T for $\sigma = 2$ is noticeably smaller than that for $\sigma = 8$. Despite this difference, both results are obviously not the flat temperature profiles found in integrable systems [39, 40]. Therefore, here the (quasi-)integrable dynamics is excluded.

Figures 1(c,d) show the result of $\kappa(L)$. As usual, $\kappa \sim L^\alpha$ is observed. This is the case for $\sigma = 2$ for the entire considered range of L , while for $\sigma = 8$ the asymptotic behavior can only be achieved for large L as the crossover to the NN interaction model. Indeed, the best fitting gives $\alpha = 0.34 \pm 0.01$, which is close to the prediction of $\alpha = \frac{1}{3}$ in FPU chains with NN interaction [46] and within the recent two predicted universality classes [25, 26]. In

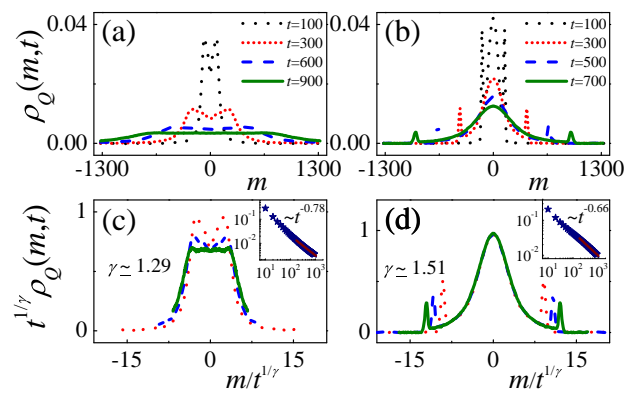


FIG. 2: $\rho_Q(m, t)$ for several t for $\sigma = 2$ (a) and 8 (b). (c) and (d) give the corresponding rescaled $\rho_Q(m, t)$ [as $t^{1/\gamma} \rho_Q(m/t^{1/\gamma}, t)$]. The inset shows $\rho_Q(0, t)$ vs t to derive the exponent γ .

contrast, for $\sigma = 2$, we obtain an enhanced κ (at least one order of magnitude compared to $\sigma = 8$ for the same L) and a quite large α ($\simeq 0.71$). We note that our estimation is convincing as it is already at a very large scale ($N = 16384$). In fact, such calculations for only the last points of Figs. 1(c,d) take one month of CPU time by an intel Xeon E5-2697v4 core even with the FFT technique [45]. We emphasize that this α , even larger than usual, is clearly at variance with $\alpha = 1$, again supporting the system's nonintegrable dynamics. More-importantly, this larger α indicates a higher thermal conductivity, undoubtedly of potential applications.

V. UNDERLYING MECHANISMS

A. New heat diffusion process

We explore this new exponent's underlying mechanisms from the following three aspects. First, a new heat diffusion process is revealed. This is exhibited in the propagation of heat fluctuations following a new shaped density with a new scaling. To characterize such process, we employ the equilibrium spatiotemporal correlation function [47, 48]

$$\rho_Q(m, t) = \frac{\langle \Delta Q_{l+m}(t) \Delta Q_l(0) \rangle}{\langle \Delta Q_l(0) \Delta Q_l(0) \rangle} \quad (3)$$

of local thermal energy $Q_l(t) = E_l(t) - \frac{\langle (E) + \langle F \rangle \rangle g_l(t)}{\langle g \rangle}$. Here, due to the translational invariance, the correlation depends only on the relative distance m ; $\langle \cdot \rangle$ represents the spatiotemporal average; l labels a coarse-grained bin's number similar to that adopted in the RNEMD method (each bin has $n = 8$ particles). In the definition of $Q_l(t)$, $g_l(t)$ is the particle number density, $E_l(t) = \sum_k E_k(t)$ with $E_k = \frac{p_k^2}{2} + \frac{1}{2}(x_{k+1} - x_k)^2 + \frac{1}{4} \sum_{j \neq k}^N \frac{(x_j - x_k)^4}{|j - k|^\sigma}$ is the energy density (note that here $\sigma' = \infty$ and the sum runs over all particles within bin l), and $F_l(t) (\langle F \rangle \equiv 0)$

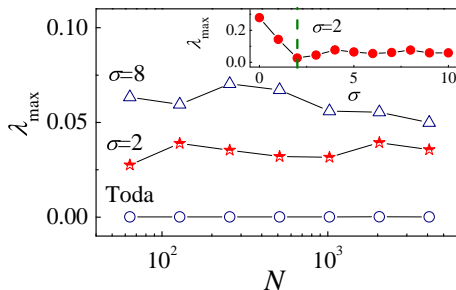


FIG. 3: λ_{\max} vs system size N for Toda chain, $\sigma = 2, 8$ (from bottom to top). The inset shows λ_{\max} vs σ .

is the pressure density, respectively. To evaluate these densities, one can calculate the number of particles $g_l(t)$, the total energy $E_l(t)$ in the bin, and the pressure $F_l(t)$ exerted on the bin, in each time t . Note that since the system is one dimensional the pressure is equal to the force and can be computed from the gradient of the potential.

Figures 2(a,b) depict $\rho_Q(m, t)$ for several t . The calculations are performed under several equilibrium states of $T = 0.5$ and $N = 4096$. For $\sigma = 8$, as usual there are Lévy walk-like profiles [49] with a slowly relaxed central peak together with two ballistically moving side peaks [see Fig. 2(b)], like what is observed in the SR interacting models. In contrast, for $\sigma = 2$, $\rho_Q(m, t)$ shows a new shape [see Fig. 2(a)]. Remarkably, the central peak for a long time now turns to a platform, indicating a much faster relaxation. We have verified that the short time's $\rho_Q(m, t)$ behaves similarly to that shown in ballistic transport [21], however our long-time scaled dynamics does support superdiffusive transport. Therefore, thanks to excluding the Kac scaling factor, the real regime of transport is revealed.

We figure out this new sort of transport by studying $\rho_Q(0, t)$ with t (see the insets of Fig. 2). It shows a good scaling $\rho_Q(0, t) \sim t^{-1/\gamma}$ with $\gamma \simeq \frac{1}{0.78} \simeq 1.29$, in contrast to $\gamma \simeq \frac{1}{0.66} \simeq 1.51$ for $\sigma = 8$. With this, the rescaled $\rho_Q(m, t)$ is plotted by

$$t^{1/\gamma} \rho(m, t) \simeq \rho(t^{-1/\gamma} m, t). \quad (4)$$

This scaling formula is based on Lévy walk theory [49]. As shown, it is well satisfied for $\sigma = 8$ (especially the central parts). For $\sigma = 2$ [see Fig. 2(c)], to see an excellent collapse requires a much longer time. However, this does not preclude the use of such a formula. In fact, another relation $\alpha = 2 - \gamma$ [49] based on the same theory connecting γ to α just gives an excellent estimation $\alpha \simeq 2 - 1.29 = 0.71$, in agreement with our above thermal conduction calculation.

B. System's weaker nonintegrability

Second, $\alpha \simeq 0.71$ seemingly relates the system's weaker nonintegrability. The nonintegrability is featured by the

maximal Lyapunov exponent $\lambda_{\max} (> 0)$ (see Fig. 3), obtained from the standard Benettin-Galgani-Strelcyn technique [50]. As a comparison, another completely integrable Toda chain [40, 51] with $\lambda_{\max} = 0$ is also demonstrated. As shown, λ_{\max} for $\sigma = 2$ just lies in between the results of $\sigma = 8$ and the Toda chain, and this seems unchanged with further increasing system size. It thus indicates the system's weaker nonintegrability compared to the counterpart SR interacting systems. Indeed, the nonmonotonic variation of λ_{\max} on σ (see the inset) also confirms this [19], but the integrable dynamics are certainly ruled out. Therefore, a weaker nonintegrability seems to provide a mechanism to raise the divergent exponent.

C. Peculiar dynamics of traveling DBs

Third, we conjecture that this weaker nonintegrability makes the system support a new type of excitations—the tail-free traveling DBs [41]—and it is these moving DBs together with their relatively weak interactions that contribute to the higher divergence. To verify this is interesting but usually greatly challenging since it is hard to catch out these moving excitations at equilibrium states due to their mobility. Viewing this we choose to first present the dynamics of moving DBs in zero-temperature systems (see Fig. 4). This is explored by using the following ansatz [52]:

$$x_j(t) = \frac{(-1)^j A_{\text{DB}} \cos[\omega_{\text{DB}} t + v_{\text{DB}}(j - x_0)]}{\cosh[\theta_{\text{DB}}(j - x_0 - v_{\text{DB}} t)]}. \quad (5)$$

Here A_{DB} (ω_{DB} ; v_{DB} ; θ_{DB}) parametrizes DB's amplitude (frequency; velocity; inverse width), and x_0 is the initial position of the DB. For a standing DB with $v_{\text{DB}} = 0$, one can set A_{DB} and find θ_{DB} using a trial and error method [52], which minimizes the oscillations of A_{DB} . As soon as θ_{DB} has been obtained, we then calculate ω_{DB} . This gives a general relation for both ω_{DB} and θ_{DB} versus A_{DB} [see Figs. 4(a,b)]. The moving DB can then be excited by applying Eq. (5) as the initial condition for the chosen A_{DB} and v_{DB} . As examples, we measure several DBs' real propagations under $A_{\text{DB}} = 1.6$ for several v_{DB} [see Figs. 4(c,d)]. As shown, DBs for $\sigma = 2$ can move freely for all studied initial v_{DB} , but in contrast, the velocities of DBs for $\sigma = 8$ decrease and they can stop. This clearly demonstrates the distinction of DBs between $\sigma = 2$ and 8.

We secondly study the spatiotemporal evolutions of local energy densities $E_i(t)$ under equilibrium states for two timescales ($t = 100$ and 1000) to visualize DBs' interactions in finite-temperature systems (see Fig. 5). The evolutions are obtained by considering a short chain with $N = 200$. The chain is first thermalized to $T = 0.5$; then the thermal baths are removed and the results are recorded and displayed by a suitable time step [$\Delta t = 1(10)$ for $t = 100(1000)$]. As indicated, both the $\sigma = 2$

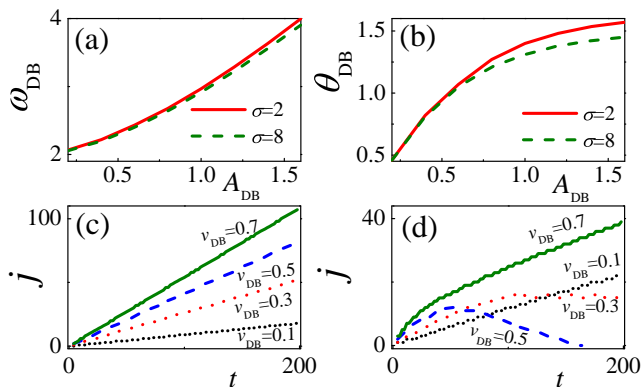


FIG. 4: ω_{DB} (a) and θ_{DB} (b) vs A_{DB} . DB's coordinate j vs t for $\sigma = 2$ (c) and 8 (d) for several v_{DB} for $A_{DB} = 1.6$.

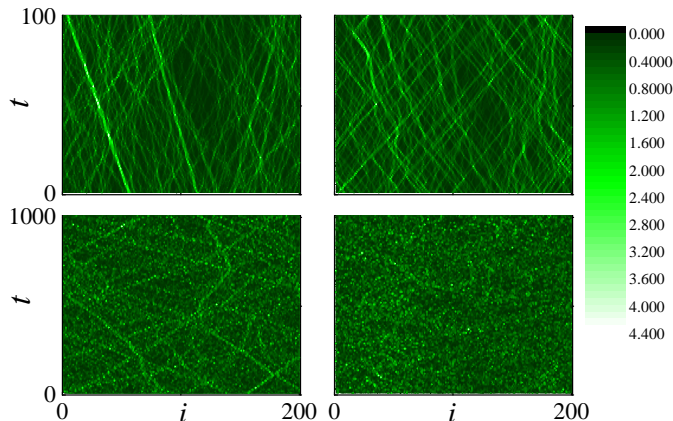


FIG. 5: Spatiotemporal evolution of energy densities $E_i(t)$ at thermal equilibrium. Left (right) panels: $\sigma = 2$ (8). Upper (lower) panels: short ($t = 100$) [long ($t = 1000$)] time with time step $\Delta t = 1$ (10).

and 8's short timescale dynamics exhibit transport similar to the ballistic regime. This explains the ballistic scaling observed in a short time. In contrast, for a relatively long-time scale, the ballistic transport for $\sigma = 8$ disappears, suggesting strong interactions between heat carriers. But this is apparently not the case for $\sigma = 2$: the signature of the localized excitations is still recognized, but probably due to their weak interactions, their identification now becomes weaker. Both dynamics in zero- and finite-temperature systems are in good accord with our conjecture.

VI. CONCLUSION

To summarize, we have revealed the intrinsic feature of thermal transport in a LR interacting system. As such we have shown that a theoretical model of the LR interacting FPU chain (with Born-von Karman periodic boundary conditions and under an appropriate range value $\sigma = 2$) can support a higher length-divergent exponent $\alpha \simeq 0.71$ of the thermal conductivity. This finding is of funda-

mental importance as it provides a theoretical possibility to search for higher thermal conductivity in 1D materials involving LR interactions, thus pointing towards new manipulations of heat in practice [33, 34]. It also opens up new avenues for exploring thermal transport as the new divergence surely indicates new mechanisms.

The higher α is related to the system's more rapid heat propagation, weaker chaotic dynamics, and also the new dynamics of traveling DBs (we have also measured the system's equilibrium heat current auto-correlation function, which supports this higher α as well [see Appendix B]). A new shaped heat propagating density is found and its scaling $\gamma \simeq 1.29$ can be well connected to α by the formula $\alpha = 2 - \gamma$ [49]. This seems to indicate that the Lévy walk model, of appropriate variations, is still useful for understanding transport in LR interacting systems. The system's weaker nonintegrability is confirmed. This suggests that although the system's chaotic dynamics is not an ingredient sufficient for the validity of Fourier's law [15], the strength of nonintegrability does influence the system's thermal conduction, thus paving a new way to use nonlinearity to control transport. More-interestingly, this weaker nonintegrability can result in peculiar dynamics of traveling DBs at thermal equilibrium and this seems responsible for the higher α . All of these would undoubtedly encourage further studies of thermal transport.

Final remark: As our finding ($\alpha \simeq 0.7$) obviously deviates from those ($\alpha = 1$, ballistic transport) in [19] by a different protocol of simulations in a FPU chain with fixed boundary conditions and currently it is difficult to evaluate whether the results from both protocols are actually equivalent, one might reconsider this issue in the future.

Acknowledgments

D.X. would like to acknowledge many helpful discussions with Prof. R. Livi and Prof. S. Lepri. This work is motivated by their excellent relevant studies. D.X. is supported by NNSF (Grant No. 11575046) of China and NSF (Grant No. 2017J06002) of Fujian Province, China. J.W. is supported by NNSF (Grant No. 11847015) of China and the start-up fund from Jiangxi Science and Technology Normal University (Grant No. 2017BSQD002). S.V.D. is supported by the Russian Foundation for Basic Research (Grant No. 19-02-00971).

Appendix A: FPU model with both quadratic and quartic LR interactions

Including the LR interactions also in the quadratic term, i.e., setting $\sigma = \sigma' = 2$ in Hamiltonian (1), will not violate our general conclusion. To demonstrate this, we here present the relevant results for heat propagation in Fig. 6. As can be seen, $\rho_Q(m, t)$ in Fig. 6(a) shows similar

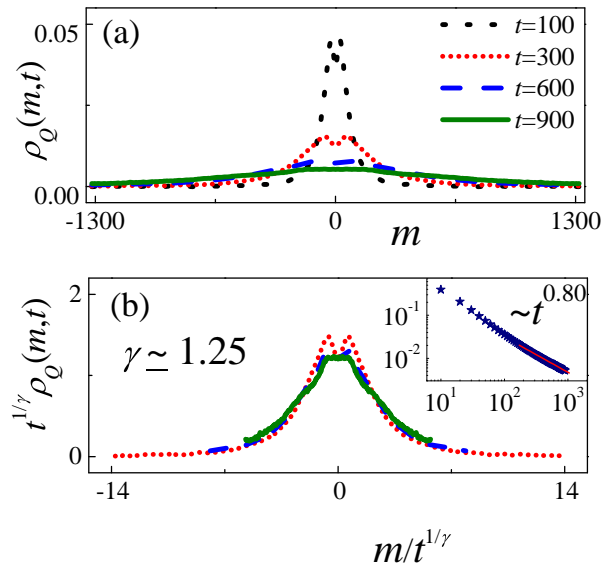


FIG. 6: (a) $\rho_Q(m,t)$ for several t for $\sigma = \sigma' = 2$. (b) gives the corresponding rescaled $\rho_Q(m,t)$ indicating $\gamma \simeq 1.25$. The inset in (b) shows $\rho_Q(0,t)$ vs t to obtain γ .

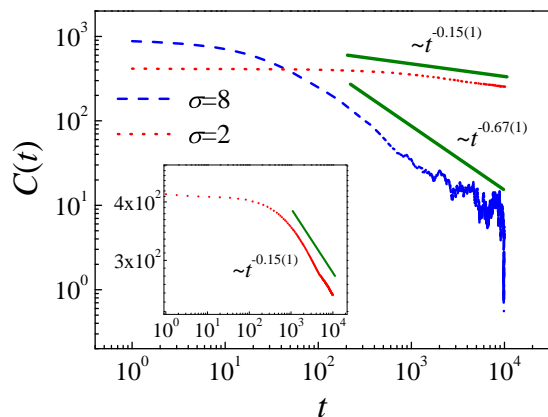


FIG. 7: The equilibrium heat current auto-correlation $C(t)$ vs t for $\sigma = 2$ and 8 . The inset is a zoom for the result of $\sigma = 2$.

shapes to those in Fig. 2(a). A slight difference is that, to clearly see the platform, longer times are required. A scaling analysis of $\rho_Q(m,t)$ for different t indicates an

exponent $\gamma \simeq 1.25$ implying $\alpha \simeq 2 - 1.25 = 0.75$. This α value is close to $\alpha \simeq 0.71$ as reported in the main text.

Appendix B: Equilibrium heat current auto-correlation

At present, there are three main approaches to detect anomalous thermal transport behavior, i.e., (i) the direct nonequilibrium molecular dynamics simulations to obtain $\kappa(L)$; (ii) the perturbation correlation method to derive $\rho_Q(m,t)$; (iii) the study of the system's equilibrium heat current auto-correlation function $C(t)$.

So far we have already shown the results of $\kappa(L)$ and $\rho_Q(m,t)$ in Figs. 1 and 2. To make our results convincing, here we provide the estimation of $C(t)$. $C(t)$ is defined by

$$C(t) = \langle J_{\text{tot}}(t) J_{\text{tot}} \rangle, \quad (\text{B1})$$

where J_{tot} is the total heat current and $\langle \cdot \rangle$ represents the equilibrium average. In the system with LR interactions like Hamiltonian (1) of $\sigma' = \infty$ and $\sigma = 2$,

$$J_{\text{tot}} = \sum_i p_i \left[x_{i+1} - x_i + \sum_{j>i} \frac{(x_j - x_i)^3}{(r_{ij})^\sigma} \right]. \quad (\text{B2})$$

The anomalous thermal transport then is related to the slow time decay of $C(t)$:

$$C(t) \sim t^{-\beta}, \quad 0 < \beta < 1. \quad (\text{B3})$$

Using the Green-Kubo formula

$$\kappa = \lim_{\tau \rightarrow \infty} \lim_{N \rightarrow \infty} \frac{1}{k_B N T^2} \int_0^\tau C(t) dt, \quad (\text{B4})$$

this slow decay leads to the diverging thermal conductivity κ .

Figure 7 depicts the results of $C(t)$ vs t for $\sigma = 2$ and 8 . For $\sigma = 8$, it indicates $\beta \simeq 0.67$, within the recent one predicted universality class of $\beta = 2/3$ [26]. In contrast, in the case of $\sigma = 2$, a slower decay ($\beta \simeq 0.15$) can be clearly identified. This suggests a new exponent of β , again supporting our findings and proposed mechanisms.

[1] S. Lepri, *Thermal Transport in Low Dimensions: From Statistical Physics to Nanoscale Heat Transfer* (Springer, International Publishing, Switzerland, 2016).
 [2] S. Lepri, R. Livi, and A. Politi, Thermal conduction in classical low-dimensional lattices, *Phys. Rep.* **377**, 1 (2003).
 [3] A. Dhar, Heat transport in low-dimensional systems, *Adv. Phys.* **57**, 457 (2008).

[4] C. W. Chang, D. Okawa, H. Garcia, A. Majumdar, and A. Zettl, Breakdown of Fourier's Law in Nanotube Thermal Conductors, *Phys. Rev. Lett.* **101**, 075903 (2008).
 [5] V. Lee, C.-H. Wu, Z.-X. Lou, W.-L. Lee, and C.-W. Chang, Divergent and Ultrahigh Thermal Conductivity in Millimeter-Long Nanotubes, *Phys. Rev. Lett.* **118**, 135901 (2017).
 [6] N. Li, J. Ren, L. Wang, G. Zhang, P. Hänggi, and B. Li,

- Rev. Mod. Phys. **84**, 1045 (2012).
- [7] F. VanGessel, J. Peng, and P. W. Chung, A review of computational phononics: The bulk, interfaces, and surfaces, *J. Mater. Sci.* **53**, 5641 (2018).
- [8] D. Segal and B. K. Agarwalla, Vibrational Heat Transport in Molecular Junctions, *Annu. Rev. Phys. Chem.* **67**, 185 (2016).
- [9] S. R. Sklan, Splash, pop, sizzle: Information processing with phononic computing, *AIP Adv.* **5**, 053302 (2015).
- [10] R. Mankowsky, M. Först, and A. Cavalleri, Nonequilibrium control of complex solids by nonlinear phononics, *Rep. Prog. Phys.* **79**, 064503 (2016).
- [11] A. Campa, T. Dauxois, D. Fanelli and S. Ruffo, *Physics of long-range interacting systems* (Oxford University Press, Oxford, 2014).
- [12] A. Campa, T. Dauxois, and S. Ruffo, Statistical mechanics and dynamics of solvable models with long-range interactions, *Phys. Rep.* **480**, 57 (2009).
- [13] F. Bouchet, S. Gupta, and D. Mukamel, Thermodynamics and dynamics of systems with long-range interactions, *Physica A (Amsterdam)* **389**, 4389 (2010).
- [14] Y. Levin, R. Pakter, F. B. Rizzato, T. N. Teles, and F. P. C. Benetti, Nonequilibrium statistical mechanics of systems with long-range interactions, *Phys. Rep.* **535**, 1 (2014).
- [15] S. Lepri, R. Livi, and A. Politi, Heat Conduction in Chains Nonlinear Oscillators, *Phys. Rev. Lett.* **78**, 1896 (1997).
- [16] S. Iubini, P. D. Cintio, S. Lepri, R. Livi, and L. Casetti, Heat transport in oscillator chains with long-range interactions coupled to thermal reservoirs, *Phys. Rev. E* **97**, 032102 (2018).
- [17] R. R. Ávila, E. Pereira, and D. L. Teixeira, Length dependence of heat conduction in (an)harmonic chains with asymmetries or long range interparticle interactions, *Physica A (Amsterdam)* **423**, 51 (2015).
- [18] C. Olivares and C. Anteneodo, Role of the range of the interactions in thermal conduction, *Phys. Rev. E* **94**, 042117 (2016).
- [19] D. Bagchi, Thermal transport in the Fermi-Pasta-Ulam model with long-range interactions, *Phys. Rev. E* **95**, 032102 (2017).
- [20] D. Bagchi, Energy transport in the presence of long-range interactions, *Phys. Rev. E* **96**, 042121 (2017).
- [21] P. D. Cintio, S. Iubini, S. Lepri, and R. Livi, Equilibrium time-correlation functions of the long-range interacting Fermi-Pasta-Ulam model, *J. Phys. A: Math. Theor.* **52**, 274001 (2019).
- [22] S. Tamaki and K. Saito, Energy current correlation in solvable long-range interacting systems, arXiv:1906.08457v1 (2019).
- [23] F. Müller-Plathe, A simple nonequilibrium molecular dynamics method for calculating the thermal conductivity, *J. Chem. Phys.* **106**, 6082 (1997).
- [24] D. Xiong, J. Wang, Y. Zhang, and H. Zhao, Nonuniversal heat conduction of one-dimensional lattices, *Phys. Rev. E* **85**, 020102(R) (2012).
- [25] H. van Beijeren, Exact Results for Anomalous Transport in One-Dimensional Hamiltonian Systems, *Phys. Rev. Lett.* **108**, 180601 (2012).
- [26] H. Spohn, Nonlinear fluctuating hydrodynamics for anharmonic chains, *J. Stat. Phys.* **154**, 1191 (2014).
- [27] M. Alaghemandi, E. Algaer, M. C Böhm, and Florian Müller-Plathe, The thermal conductivity and thermal rectification of carbon nanotubes studied using reverse non-equilibrium molecular dynamics simulations, *Nanotechnology* **20**, 115704 (2009).
- [28] B. Li, L. Wang, and B. Hu, Finite Thermal Conductivity in 1D Models Having Zero Lyapunov Exponents, *Phys. Rev. Lett.* **88**, 223901 (2002).
- [29] J. W. Britton, B. C. Sawyer, A. C. Keith, C.-C. J. Wang, J. K. Freericks, H. Uys, M. J. Biercuk, and J. J. Bollinger, Engineered two-dimensional Ising interactions in a trapped-ion quantum simulator with hundreds of spins, *Nature (London)* **484**, 489 (2012).
- [30] S. T. Bramwell, M. J. Harris, B. C. den Hertog, M. J. P. Gingras, J. S. Gardner, D. F. McMorrow, A. R. Wildes, A. Cornelius, J. D. M. Champion, R. G. Melko, and T. Fennell, *Phys. Rev. Lett.* **87**, 047205 (2001).
- [31] R. G. Melko, B. C. den Hertog, and M. J. P. Gingras, Long-Range Order at Low Temperatures in Dipolar Spin Ice, *Phys. Rev. Lett.* **87**, 067203 (2001).
- [32] R. F. Wang, C. Nisoli, R. S. Freitas, J. Li, W. McConville, B. J. Cooley, M. S. Lund, N. Samarth, C. Leighton, V. H. Crespi, and P. Schiffer, Artificial ‘spin ice’ in a geometrically frustrated lattice of nanoscale ferromagnetic islands, *Nature (London)* **439**, 303 (2006).
- [33] E. Pereira and R. R. Ávila, Increasing thermal rectification: Effects of long-range interactions, *Phys. Rev. E* **88**, 032139 (2013).
- [34] S. Chen, E. Pereira and G. Cassati, Ingredients for an efficient thermal diode, *Europhys. Lett.* **111**, 30004 (2015).
- [35] Serach *Born-von Karman boundary condition* in <https://en.wikipedia.org/wiki/>
- [36] H. Christodoulidi, C. Tsallis, and T. Bountis, Fermi-Pasta-Ulam model with long-range interactions: Dynamics and thermostatics, *Europhys. Lett.* **108**, 40006 (2014).
- [37] F. Tamarit and C. Anteneodo, Rotators with Long-Range Interactions: Connection with the Mean-Field Approximation, *Phys. Rev. Lett.* **84**, 208 (2000).
- [38] Our study of the model including LR interactions in both the quadratic and quartic terms confirms this, see Appendix A for the model’s heat propagation.
- [39] Z. Rieder, J. L. Lebowitz, and E. Lieb, Properties of a Harmonic Crystal in a Stationary Nonequilibrium State, *J. Math. Phys.* **8**, 1073 (1967).
- [40] M. Toda, Solitons and Heat Conduction, *Phys. Scr.* **20**, 424 (1979).
- [41] Y. Doi and K. Yoshimura, Symmetric potential lattice and smooth propagation of tail-free discrete breathers, *Phys. Rev. Lett.* **117**, 014101 (2016).
- [42] S. Stackhouse, L. Stixrude, and B. B. Karki, Thermal Conductivity of Periclase (MgO) from First Principles, *Phys. Rev. Lett.* **104**, 208501 (2010).
- [43] <http://lammmps.sandia.gov>
- [44] M. P. Aùllen and D. L. Tildesley, *Computer Simulation of Liquids* (Clarendon, Oxford, 1987).
- [45] S. Gupta, M. Potters, and S. Ruffo, One-dimensional lattice of oscillators coupled through power-law interactions: Continuum limit and dynamics of spatial Fourier modes, *Phys. Rev. E* **85**, 066201 (2012).
- [46] O. Narayan and S. Ramaswamy, Anomalous Heat Conduction in One-Dimensional Momentum-Conserving Systems, *Phys. Rev. Lett.* **89**, 200601 (2002).
- [47] H. Zhao, Identifying Diffusion Processes in One-

- Dimensional Lattices in Thermal Equilibrium, Phys. Rev. Lett. **96**, 140602 (2006).
- [48] S. Chen, Y. Zhang, J. Wang, and H. Zhao, Diffusion of heat, energy, momentum, and mass in one-dimensional systems, Phys. Rev. E **87**, 032153 (2013).
- [49] V. Zaburdaev, S. Denisov, and J. Klafter, Lévy walks, Rev. Mod. Phys. **87**, 483 (2015).
- [50] A. Pikovsky and A. Politi, *Lyapunov exponents: a tool to explore complex dynamics* (Cambridge University Press, Cambridge, 2016).
- [51] To facilitate the simulations, we use such a Hamiltonian:

$$H = \sum_i \frac{p_i^2}{2} + \exp(x_i - x_{i+1}) + x_{i+1} - x_i - 1.$$
- [52] D. Xiong and S. V. Dmitriev, Effects of Discrete Breathers on Thermal Transport in the ϕ^4 Lattice, in *A Dynamical Perspective on the ϕ^4 Model*, edited by P. Kevrekidis and J. Cuevas-Maraver (Nonlinear Systems and Complexity, vol 26. Springer, Cham, 2019).